

Hands on Experiment-XENON1T : Characterization of R11410 PMTs

Ander Simón Estévez^a, Susnata Seth^{b*}, Andrea Molinario^c, Rino Persiani^d and Alfredo Davide Ferella^c

^a *Instituto de Física Corpuscular (IFIC), CSIC-UV, Valencia*

^b *Astroparticle Physics and Cosmology Division, Saha Institute of Nuclear Physics, 1/AF Bidhannagar, Kolkata 700 064, India*

^c *INFN-Laboratori Nazionali del Gran Sasso, Assergi, 67010, Italy*

^d *University of Bologna and INFN-Bologna, Bologna, Italy*

*E-mail: ander.simon@ific.uv.es, susnata.seth@saha.ac.in,
andrea.molinario@lngs.infn.it, rino.persiani@bo.infn.it,
alfredo.ferella@lngs.infn.it*

XENON is a dark matter direct detection experiment. It uses a dual phase (liquid-gas) xenon filled time projection chamber to observe of nuclear recoils induced by Weakly Interacting Massive Particles, measuring two scintillation signals. XENON1T, the next generation detector with a ton scale mass, is being installed at Gran Sasso National Laboratory in Italy. R11410 photomultiplier tubes produced by Hamamatsu will be used for detection of scintillation lights. The characterization of such devices has been performed during the summer school and the results of the study are discussed here.

*Gran Sasso Summer Institute 2014 Hands-On Experimental Underground Physics at LNGS - GSSI14, 22 September - 03 October 2014
INFN - Laboratori Nazionali del Gran Sasso, Assergi, Italy*

*Present E-mail: susnata.seth@tifr.res.in, Present Address: Tata Institute of Fundamental Research, 1st Homi Bhabha Road, Colaba, Mumbai 400 005, India.

1. Introduction

The XENON project is based on a series of experiments searching for cold dark matter through the direct detection of Weakly Interacting Massive Particles (WIMPs). All the XENON detectors are based on dual phase (liquid-gas) xenon filled Time Projection Chambers (TPCs). XENON100 is the current generation experiment located at the Laboratori Nazionali del Gran Sasso (LNGS) in Italy [1]. It has been running since 2009 and it set one of the best limit to WIMP-nucleon cross section to date [2]. The next generation detector (of ton-scale mass) of the XENON project is XENON1T which is currently being installed at LNGS.

TPC contains the xenon liquid with a layer of xenon gas at its top. The passage of an incoming particle can give rise to two scintillation signals. An energy deposition in the liquid xenon produces both, ionization and excited atoms. While the de-excitation of atoms gives a prompt scintillation photons (S1), the ionized electrons are drifted towards the liquid-gas interface from their interaction sites by a strong homogeneous electric field. As a result those are extracted from liquid Xe and during passing through the gas again produce a delayed scintillation lights (S2). Both of the signals are detected by an array of PMTs, one array is immersed in the liquid Xe below the cathode of the TPC and other array is placed in the xenon gas.

The reconstruction of the three-dimensional position of the interaction site and the estimation of the energy deposition in the detector can be obtained from the S1 and S2 signals of each event. The time difference between these two signals multiplied by electron drift velocity gives the depth of the interaction in the TPC. The (x, y) position of the interaction site is obtained from the hit patterns of S2 signal on the PMTs in the gas phase. The S1 signal is used to estimate the energy deposited in the detector. The ratio S2/S1 is lower for nuclear recoil induced events than electron recoil induced ones, thus allowing discrimination between β and γ induced events (which preferably give rise to electron recoils than nuclear recoils) from those induced by neutrons, WIMPs. As a result, the characterization of PMTs becomes essential to obtain all the above mentioned estimation precisely. In this paper we present the characterization of PMTs.

2. PMTs Characterization

In XENON1T detector the detection of scintillation light will take place with an array of PMTs Hamamatsu R11410. These devices consist of three main parts: a photocathode, an amplification chain with a series of dynodes and an anode. An electrical potential of order 1.5 kV is applied between the photocathode and the anode. When a photon hits the photocathode, a photoelectron can be emitted. This is accelerated by the applied electric field and hits the first dynode, where it gets multiplied by a certain gain factor. At each stage in the amplification chain a new multiplication occurs. The produced electrons are eventually collected on the anode. Under real circumstances number of photons falling on photocathode is not constant. In addition, emission of photoelectrons and their subsequent collection by dynode process are also random binary process. As a result, the probability of observing n photoelectrons with their mean at μ can be expressed by a Poisson distribution,

$$P(n, \mu) = \frac{\mu^n e^{-\mu}}{n!}. \quad (2.1)$$

The aim of our work is to perform measurement of the gain of PMTs and also to find the impurities in the PMTs. The estimation of the gain of the PMTs is performed by conducting experiment as well as with the help of Monte Carlo simulation.

2.1 Experimental Setup

We used a light emitting diode (LED) as a pulsed source of light. A blue light from LED went inside a closed chamber through optical fiber and two PMTs were used to collect that light (shown in figure 1). Light pulse was generated with Lecroy 9211 pulse generator and the external trigger was synchronized with LED light emission. We performed our measurements driving the LED with pulses of different voltages, namely 2.3 V, 3.0 V, 3.5 V and 4.0 V, and width of 20 ns. Signals from the PMTs were digitized using CAEN V1724 digitizers, 14 bit, 0.5 V_{pp}, 100 MS/s. We acquired 10⁴ events for each pulse voltage. We also acquired data with input voltages of LED of values 4.5 V and 5.0 V with time width 40 ns and 50 ns respectively.

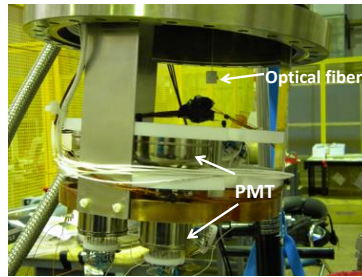


Figure 1: The optical fiber through which light went to the closed chamber and the PMTs are shown.

2.2 Signal preprocessing

In order to determine the baseline, the distribution of ADC channel has been plotted for each PMT. In figure 2 (left) a typical distribution of ADC channel is shown. The peak of the distribution was fitted by a Gaussian function and the mean of the Gaussian function was taken as the value of baseline.

With this, signal identification was made by looking for a minimum inside a 100 ns fixed window. We expect that the signals always fall inside this fixed time window because of the synchronization between external trigger and LED light emission.

The last step is to calculate the whole charge produced by the light in the PMT. First we calculate for each sample the amplitude V of the signal expressed in mV, which is given by the difference between the ADC channel value and the baseline multiplied by the conversion factor of 0.03 mV/chan. This amplitude is integrated inside the 100 ns signal window, obtaining the value V_{int} . We then calculate the charge Q inside the signal window as

$$Q = \frac{V_{int}}{Z} \quad (2.2)$$

where $Z = 50\Omega$ is the impedance of digitizer.

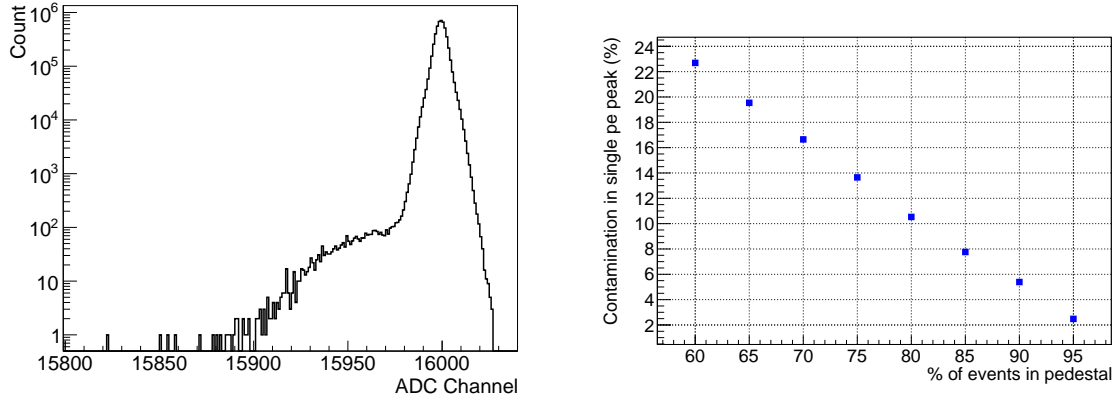


Figure 2: Distribution of ADC signal of a PMT (left). Contamination percentage in events with detected photoelectrons as function of the fraction of pedestal events (right).

2.3 Determination of the gain of PMT

The gain of a PMT can be determined measuring the number of electrons collected on the anode when a single photoelectron is emitted by the photocathode. This means that, in order to perform an optimal measurement of the gain of a PMT, we have to put ourselves in a condition as close as possible to the one where only 0 or 1 photoelectrons are produced. Looking at number of events with respect to the total belonging to the pedestal peak (figure 3 left), which corresponds to 0 photoelectrons, we get the mean μ of the number of emitted photoelectrons. Using Poisson distribution (2.1) with mean μ we can calculate the contamination c , that is the percentage of events where $n \geq 2$ photoelectrons are produced. We consider acceptable a contamination of $c \leq 5\%$, which happens when $>90\%$ of the total events are in the pedestal peak (figure 2 right).

Quick data acquisitions with several voltages showed that the operating voltage for the LED that implied a 5% contamination was 2.3V with a width of the emitting pulse of 20 ns. This is the value chosen to measure the gain of each PMT. The distributions of charge obtained with this voltage for a PMT is shown in the figure 3 (left).

Each distribution contains two peaks. The larger peak centered in zero is the so called pedestal peak and is due to noise, while the smaller peak is expected to be created by the single photoelectron or superposition of single and multiple photoelectrons. In our experiment we have assumed that the second peak is a superposition of single and two photoelectrons. So, the charge distribution has been fitted by an equation which is combination of three Gaussian functions (shown in figure 3 (left)) and can be expressed as,

$$f(x) = p_0 \exp\left(-\frac{(x-p_1)^2}{2p_2^2}\right) + p_3 \exp\left(-\frac{(x-p_4)^2}{2p_5^2}\right) + p_6 \exp\left(-\frac{(x-2p_4)^2}{4p_5^2}\right) \quad (2.3)$$

where x represents charge in pC and p_0 to p_6 are the parameters of the fit. The gain of a PMT can be calculated by the following relation,

$$\text{Gain} = \frac{\text{Charge related to single photoelectron peak}}{\text{Charge of electron}} \quad (2.4)$$

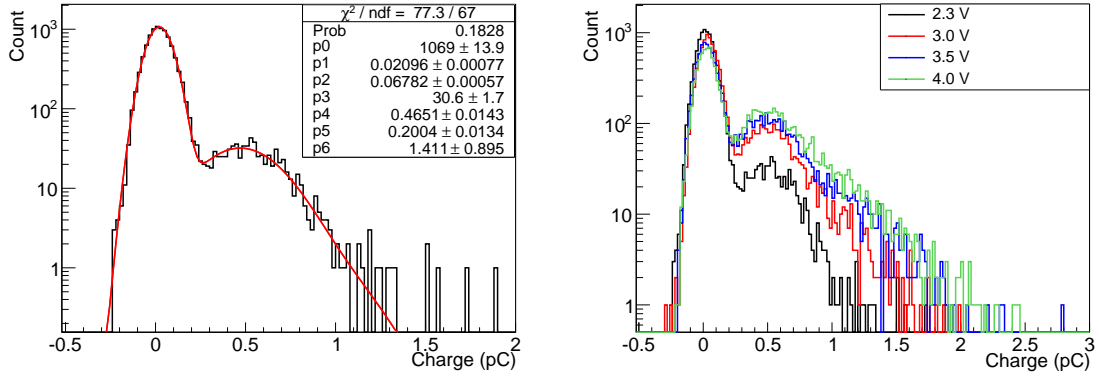


Figure 3: Distributions of charge of photoelectrons for a PMT (left). Distributions of charge for different input voltage to the LED (right).

This means that the mean of the Gaussian for the single photoelectron, p_4 , is the parameter to be used to calculate the gain. The gain of PMT1 and PMT2 were estimated to be about $(2.90 \pm 0.06) \times 10^6$ and $(2.03 \pm 0.07) \times 10^6$, respectively.

Even though the calculation of the gain is best with lower contamination, it can be checked that the gain doesn't vary with the light intensity. The charge distribution for four different LED voltages is shown in figure 3 (right).

2.4 Simulation of the PMT response

The response of the PMTs can be easily simulated thanks to the Poisson nature of the detection process of the sensor. This simulation consists of having a random number of initial photoelectrons following a Poisson distribution and applying a multiplication factor for each of the 12 dynodes of the PMT. This factor also follows a Poisson distribution with mean equal to the gain of the dynode. Finally, we only have to add the Gaussian noise of the pedestal to the number of photoelectrons calculated.

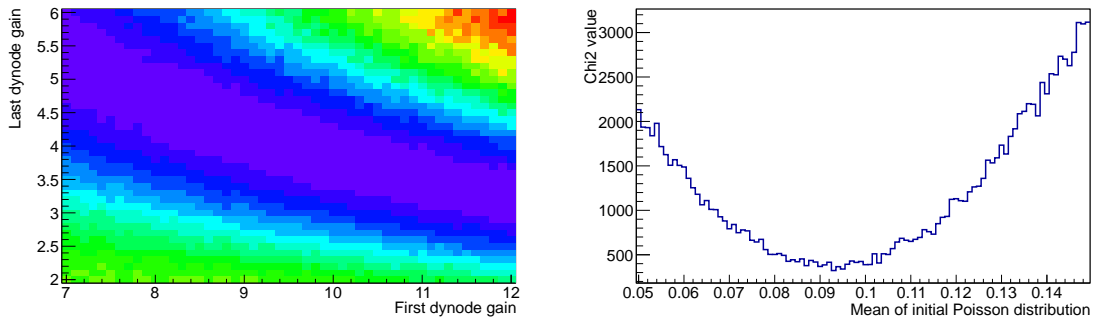


Figure 4: χ^2 distribution in function of both the first and last dynode gains (left) and in function of the mean value of the initial number of photoelectrons (right).

With this approach one could easily calculate all the parameters of a PMT comparing the response of the sensor with the response given by the simulation and minimizing χ^2 . However, having so many free parameters would imply an unreasonable enormous processing time. We decided to leave as free parameters both the first dynode gain, as it impacts greatly the shape and position of the single photoelectron peak, and the last one, as it can be used as fine-tuning. The other gains from the dynodes were fixed to 3 except the second one which, after some testing, was fixed to 3.8. In addition, the starting number of photoelectrons was set to a reasonable number of 0.1 (the voltage was set to have a 90% of pedestal events) and the pedestal peak width was fixed to the value obtained during the gain calculation, 0.06 pC.

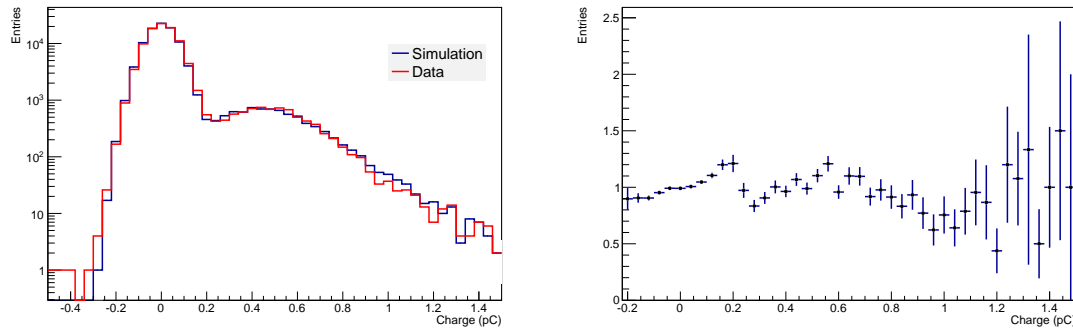


Figure 5: Comparison between simulated and measured response of the PMT (left). Ratio bin per bin of the two spectrums (right).

With this, as showed in figure 4, the best match between data and simulation response was achieved for gains of 8.7 and 4.4 for the first and last dynode respectively. After that one could fix those parameters and free the mean of the initial number of photoelectrons in order to get a more precise value. This value, showed in figure 4 (right), is 0.093.

Finally, we can compare the spectra of the data and the simulation with the estimated parameters. As showed in figure 5, the spectra fits greatly with a ratio bin per bin centered at one. The higher charge bins doesn't fit properly because of low statistics.

2.5 Afterpulse measurement

Afterpulses are signals following the main light detection. This phenomenon happens because of gas impurities inside the PMT volume. These impurities are ionized by the electron cascade due to photon detection and get accelerated by the electric field. They hit the dynodes chain giving rise to electronic multiplication and finally to the delayed signal.

While the probability of having afterpulse depends only on the prompt signal causing the effect, the time difference between the prompt signal and the afterpulse only depends on the working voltage of the PMT and on the molecular mass of the impurities, this means the delay between signals is fixed for a given impurity and a fixed voltage. This feature implies the ability of doing mass spectroscopy of the impurities inside PMT.

With this in mind and using reference values calculated by the XENON collaboration we have managed to identify the impurities of our PMT. In figure 6 you can see how the same peaks appear

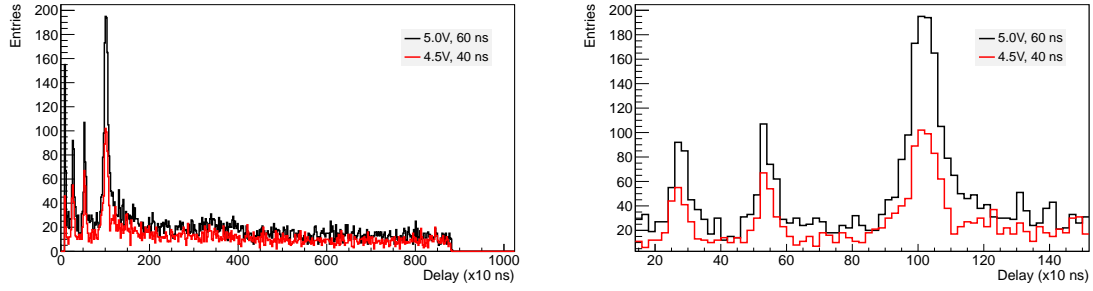


Figure 6: Difference between peak position and the position of the minimum ADC after the light peak. The peaks correspond to hydrogen (270 ns), helium (535 ns) and methane (1 μ s).

for two different light pulses. These peaks are centered in 270 ns (hydrogen), 535 ns (helium) and 1 μ s (methane).

3. Conclusions

In summary, we have studied the response from the PMT R11410 which will be used for detection of scintillation lights in XENON1T experiment. The gain was estimated by fitting the charge distribution of photoelectrons. This result provides a good agreement with the outcomes of MC simulation of the amplification chain. The analysis of afterpulsing provides detailed information of the impurities inside the PMTs.

References

- [1] E. Aprile *et al.* [XENON100 Collaboration], *Astropart. Phys.* **35** (2012) 573 [arXiv:1107.2155 [astro-ph.IM]].
- [2] E. Aprile *et al.* [XENON100 Collaboration], *Phys. Rev. Lett.* **109** (2012) 181301 [arXiv:1207.5988 [astro-ph.CO]].